

Fully broadband vAPP coronagraphs enabling polarimetric high contrast imaging

Steven P. Bos^a, David S. Doelman^a, Jos de Boer^a, Emiel H. Por^a, Barnaby Norris^b, Michael J. Escuti^c, and Frans Snik^a

^aLeiden Observatory, Leiden University, P.O. Box 9513, 2300 RA Leiden, The Netherlands

^bSydney Institute for Astronomy (SifA), Institute for Photonics and Optical Science (IPOS), School of Physics, University of Sydney, NSW2006, Australia

^cDepartment of Electrical and Computer Engineering, North Carolina State University, Raleigh, NC 27695, USA

ABSTRACT

We present designs for fully achromatic vector Apodizing Phase Plate (vAPP) coronagraphs, that implement low polarization leakage solutions and achromatic beam-splitting, enabling observations in broadband filters. The vAPP is a pupil plane optic, inducing the phase through the inherently achromatic geometric phase. We discuss various implementations of the broadband vAPP and set requirements on all the components of the broadband vAPP coronagraph to ensure that the leakage terms do not limit a raw contrast of 10^{-5} . Furthermore, we discuss superachromatic QWPs based of liquid crystals or quartz/MgF2 combinations, and several polarizer choices. As the implementation of the (broadband) vAPP coronagraph is fully based on polarization techniques, it can easily be extended to furnish polarimetry by adding another QWP before the coronagraph optic, which further enhances the contrast between the star and a polarized companion in reflected light. We outline several polarimetric vAPP system designs that could be easily implemented in existing instruments, e.g. SPHERE and SCE_xAO.

Keywords: coronagraphy, polarimetry, high contrast imaging

1. INTRODUCTION

High contrast imaging instruments investigate the circumstellar region direct around the star to search for exoplanets and signs of planet formation. One of the most exciting goals is the direct imaging and characterization of Earth-like exoplanets to search for signs of life. This is incredibly hard as an Earth-like exoplanet around a Sun-like star at 50 pc will have an angular separation of ~ 50 mas and in the visible a contrast of $\sim 10^{-10}$. This requires suppression of the diffracted starlight, many orders of magnitude brighter than the emitted light or reflected starlight from the exoplanet, with a coronagraph. Adaptive optics (AO) systems on ground-based systems are unable to give a perfect correction to wavefront distorted by the atmosphere, and therefore the raw contrast achievable by coronagraphs at small inner working angles (IWA) is fundamentally limited to $\sim 10^{-5}$.¹ The raw contrast will be further degraded by quasi-static aberrations originating from within the telescope and instrument, e.g. due to changes in temperature and gravitational vector. To reach the contrast required for Earth-like exoplanets, diversity between the light from the star and planet has to be utilised. Techniques such as angular differential imaging² (ADI) and spectral differential imaging³ (SDI) are very successful, but have a reduced effectiveness at small IWA when the diversities they rely on diminish in these regions. High-dispersion ($R \sim 100,000$) spectroscopy³ (HDS) and polarimetric differential imaging⁴ (PDI) are techniques capable of increasing contrast at small IWA.

The Apodizing Phase Plate^{5,6,7} (APP) is a transmissive optic that sculpts a 180° dark hole in the point spread function (PSF) from 2 to $7 \lambda/D$ at one side of the star and generally gives a 10^{-4} contrast. The APP applies a phase in the pupil plane by optical path differences (OPD) caused by the varying height of a diamond

email: stevenbos@strw.leidenuniv.nl

turned zinc selenide plate. Being a pupil plane coronagraph makes the APP robust against tip-tilt errors and resolved stars,⁸ problems that focal plane coronagraphs limit in performance. The diamond turning process is the limiting factor for the APP as it requires smoothly varying phase patterns that: 1) will not give the optimal contrast and strehl performance, 2) only allow for 180° dark holes requiring two observations to investigate the full circumstellar region, and 3) is very chromatic due to the wavelength dependence of the OPD.

The vector APP⁹ (vAPP) solves these problems by inducing the phase through the geometric phase^{10,11} on the circular polarization states. The vAPP is an liquid crystal plate that is an half-wave retarder with a spatially varying fast axis. The acquired phase ϕ by the \pm circular polarization states depends locally on the fast axis angle θ , and is given by $\phi = \pm 2\theta$. The geometric phase is inherently achromatic, but the efficiency of the light that acquires this phase is determined by retardance of the liquid crystal layer. Any retardance offsets from half-wave will result in leakage that did not acquire the desired phase. A direct-writing systems¹² allows for extreme fast axis orientation patterns that are required for optimally designed phase designs for arbitrary telescope apertures¹³ and 360° dark holes.¹⁴ Self aligning liquid crystal layers^{15,16} enable wave plates close to half-wave over broad wavelength ranges. The vAPP yields two PSFs with opposite circular polarization and opposite dark holes that need to be separated. The first iteration¹⁴ of the vAPP separated the two PSFs by adding a quarter-wave plate (QWP) and a polarizer (e.g. a Wollaston prism or a polarizing beam splitter cube), see [Figure 1 A](#). For the achievable raw contrast not be limited by leakage terms sets tight tolerances on the retardance and fast axis offsets of the vAPP and QWP, and the extinction ratio of the polarizer. Leakage due to retardance offsets of the half-wave liquid crystal layer imprints a copy of the non-coronagraphic in the dark holes, while leakage of similar and fast axis orientation offsets by the QWP and polarizer mixes the two coronagraphic PSFs. Another way of splitting the two PSFs and simultaneously separating the coronagraphic PSFs from the leakage PSF, is by adding a tip-tilt phase ramp to the apodizing phase pattern itself, as is shown in [Figure 1 B](#). This is known as a polarization grating¹⁷ (PG), that separates the opposite circular polarization states, and these coronagraphs are therefore known as grating vAPPs (gvAPP). Due to wavelength smearing by the grating, the gvAPPs are mainly suitable for narrowband imaging and low resolution integral field spectrographs (IFS) such as CHARIS^{18,19} and SPHERE-IFS^{20,21}. The gvAPP has already been put on sky with several instruments, e.g. SCEXAO,²² MagAO/Clio2²³ and LEXI.²⁴

The gvAPP has excellent broadband performance, but is not suitable for broadband imaging (polarimetry) or as a combination with a high resolution IFS.²⁵ For this we have to turn back to PSF splitting with QWPs and polarizers. In this proceeding we will explore how fully broadband vAPPs and polarimetric vAPPs can be implemented in existing high contrast imaging systems such as SPHERE²⁶ and SCEXAO.²⁷

2. FULLY BROADBAND VAPPS

Fully broadband vAPPs that do not suffer from wavelength smearing have different implementations depending on the symmetric (e.g. 360° vAPP) or anti-symmetric (e.g. 180° vAPP) coronagraphic PSFs. Symmetric vAPPs can benefit from a second PG with an opposite tip-tilt after a gvAPP (the double-grating vAPP²²) that folds back the PSFs back on top of each other, see [Figure 2 A](#). This has the added benefit that leakage by the vAPP is greatly reduced by the combination of the two gratings and has already be implemented²² for LMIRcam²⁸ on the LBT telescope.

Asymmetric vAPPs can also benefit from the leakage reduction by the double-grating, see [Figure 2 B](#), but still need another method to separate the PSFs, otherwise the dark hole of one PSF will be filled by the bright side of the other. To separate the PSFs we go back to the first iteration¹⁴ of the vAPP, i.e. add an QWP and polarizer downstream of the vAPP, see [Figure 1 A](#) and [Figure 2 B](#). This sets tight tolerances on the retardance and fast axis offsets of the vAPP and QWP, and the extinction ratio (ER) of the polarizer. Leakage from the vAPP will imprint a copy of the non-coronagraphic PSF and is determined by retardance offsets ($\Delta\delta$) from half-wave. Offsets of the fast axis orientation change the imprinted phase and are not considered in this work. The intensity of the leakage term (I_{HWP}) is given by:

$$I_{HWP} = \sin\left(\frac{1}{2}\Delta\delta\right)^2. \quad (1)$$

Requirements	Leakage	Retardance and fast axis angle
HWP	$< 1 \cdot 10^{-3}$	$\Delta\delta < 3.6^\circ$
QWP	$< 5 \cdot 10^{-5}$	$\Delta\delta < 0.8^\circ, \Delta\theta < 0.4^\circ$
polarizer	$< 5 \cdot 10^{-5}$	ER. $< 20.000 : 1$

Table 1. Requirements for 180° vAPPs with a raw contrast $< 10^{-5}$.

Requirements	Leakage	Retardance and fast axis angle
HWP	$< 2.5 \cdot 10^{-3}$	$\Delta\delta < 5.7^\circ$
QWP		
polarizer		

Table 2. Requirements for 360° vAPPs with a raw contrast $< 10^{-5}$.

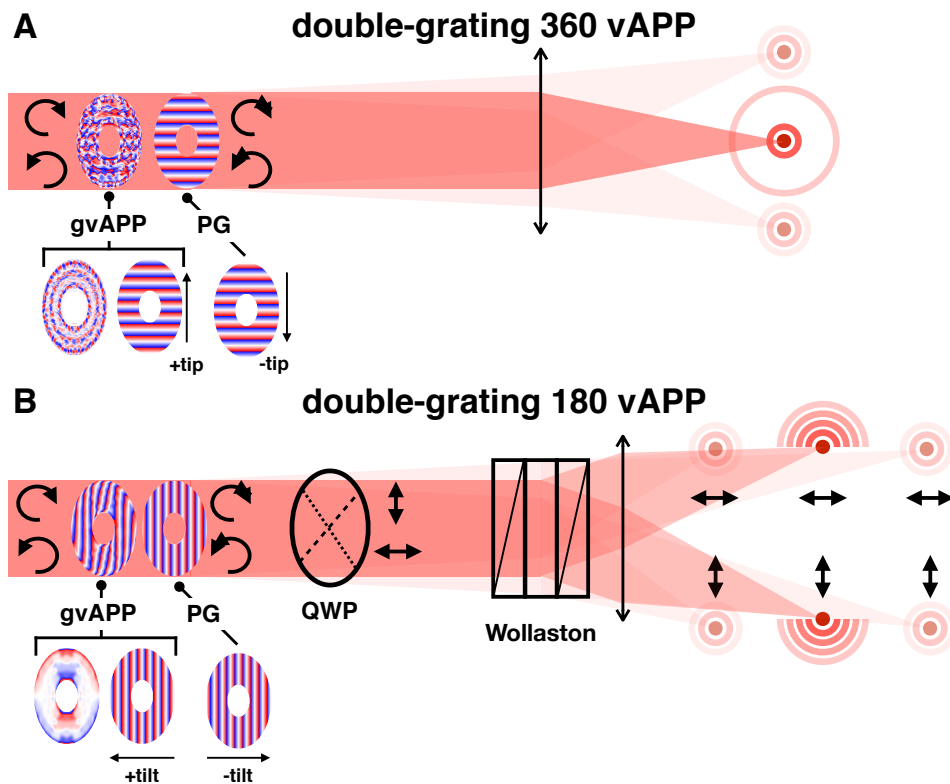


Figure 2. Double-grating implementations of (A) the 360° vAPP and (B) the 180° vAPP by combining a gvAPP with an additional polarization grating (PG) with opposite tip-tilt.

2.1 Components

Table 1 and Table 2 set the requirements on the components for a raw contrast of $< 10^{-5}$. For a broadband vAPP this means that over a sufficient wavelength range the components need to meet these requirements. The vAPP is a stack of self-aligning liquid crystal layers that have a half-wave retardance with a spatially varying fast axis orientation. Half-wave liquid crystal retarders have been fabricated with leakage of $\sim 10^{-2}$ over broad wavelength ranges in the optical¹⁵ (400-750 nm), near infrared²⁹ (900-2400 nm) and infrared²³ (2000-4500 nm). These retarders meet, combined with the double-grating technique, the leakage requirements. Furthermore, the liquid crystals have also been shown to operate in cryogenic environments.²³

The requirements for the QWP are much tighter and cannot benefit from the double-grating technique. However, there is a broader choice of materials available as the fast axis orientation constant within the optic. In the NIR an off-the-shelf superachromatic QWP (Pancharatnam configuration of three MgF2/quartz plates) provided by Thorlabs already meets the requirements over a broad (900 - 2700 nm) wavelength range. Similar wave plates in the visible and infrared off-the-shelf products that meet the requirements are currently not available. Therefore, custom QWP designs have to be pursued that might employ more MgF2/quartz plates. For MgF2/quartz retarders further investigation is needed to identify the impact of fringing, their thermal properties and wavefront quality. Liquid crystal QWPs¹⁵ are available as well that can operate in the required wavelength ranges and are less prone to fringing problems, thermal expansion and reach a satisfactory wavefront error (WFE). Further research is required to investigate if such wave plates can be fabricated that reach a satisfactory retardance and fast axis orientation performance.

The choice of polarizer mainly depends on the optical system, but polarizing beam splitters are favoured for the sake of photon efficiency. Wollaston prism are an ideal choice: high extinction ratio ($\sim 100.000:1$) and achromatic. Polarizing beam splitter cubes/plates with dielectric and/or metallic coatings (wire grid cubes suffer from high WFE in the reflected beam) combined with additional (wire grid) polarizers in the two beams to increase the polarization purity, can also reach a sufficient broadband performance.

2.2 Implementations for existing instruments

2.2.1 SPHERE-IRDIS

Within the high contrast imaging instrument SPHERE²⁶ and behind the extreme AO system SAXO³⁰ sits the NIR imaging arm IRDIS.³¹ Within this arm there are two pupil planes (pre-apodizer and Lyot) available where a broadband vAPP can be installed. The pre-apodizer wheel is preferable, because downstream there can be a focal plane mask installed that prevents saturation effects with long integration times. A double-grating 360° vAPP (see Figure 3 for the preliminary design) with a liquid crystal recipe similar to the SCEXAO gvAPP²⁹ can easily be installed. A 180° vAPP (Figure 3) requires an additional optically contacted (to the liquid crystal plate) QWP and the existing wire grid polarizers³² (if their ER is sufficient). To increase the photon efficiency, an upgrade of the existing beam splitter plate to an polarizing beam splitter plate would be favourable. A focal plane mask for the 180° would require a combination of a neutral density filter and a polarizer as the two coronagraphic PSFs still overlap.

2.2.2 SCEXAO

Similar designs can also be put in SCEXAO,²⁷ see Figure 4 for the phase designs. They could be installed in the pupil plane where the current SCEXAO gvAPP²⁹ resides. There will be Wollaston prisms installed³³ in CHARIS and in front of the CRED-2 camera that can be used for the beam-splitting of the 180° vAPP.

3. POLARIMETRIC VAPPS

As the vAPP operates on the polarization nature of light, it can be naturally combined with broadband imaging polarimetry.³⁴ A 360° vAPP as in Figure 2 A combined with a beam splitting polarizer (see Figure 5 A and B) is a dual-beam polarimetric system, as both PSFs measure an orthogonal polarization and can directly be subtracted and added due to identical morphologies of the PSFs. On the other hand, a 180° vAPP (Figure 2 B) combined with an upstream QWP is considered to be a single-beam system, see Figure 5 C, and has to be

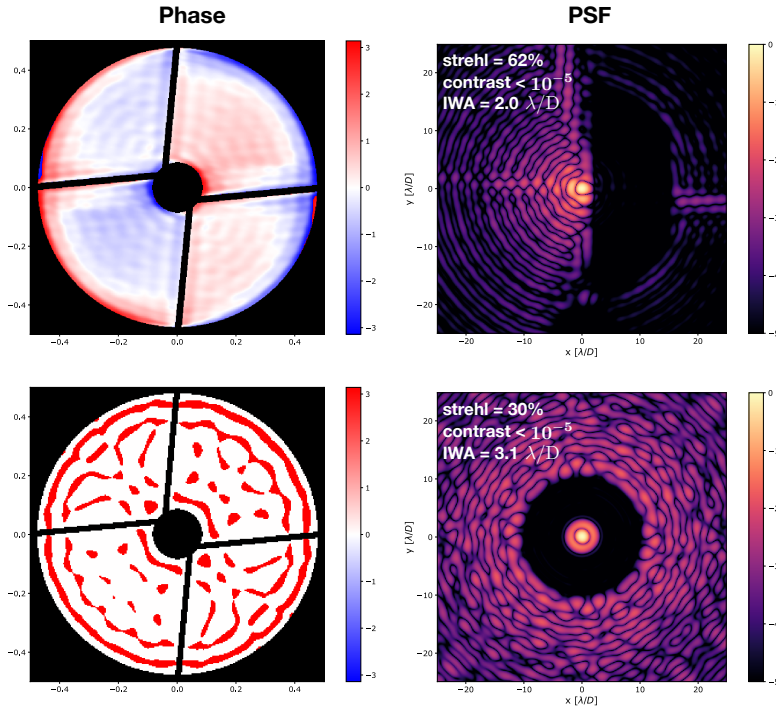


Figure 3. Preliminary 180° (top row) and 360° (bottom row) vAPP designs for SPHERE.

temporally modulated as the morphologies of the PSFs are different and cannot be subtracted or added directly. Dual-beam polarimetric 180° vAPP systems have been explored by Snik³⁴ and will not be discussed here due to the complexity of their implementation. Note that vAPPs are generally designed for a specific pupil shape and focal plane layout, therefore they can only be operated in pupil tracking mode.

The specific polarimetric implementation of the vAPP is determined by the symmetry (symmetric/anti-symmetric) of the coronagraphic PSF, the position (up- or downstream of the vAPP) and the speed (faster/slower than coherence time atmosphere) of the polarization modulator, and a single- or dual-beam implementation.⁴ Polarimetric vAPPs with asymmetric PSFs are most straightforward implemented as single-beam systems, while symmetric PSFs can simply be operated as dual-beam systems. Single-beam implementations are only possible with fast polarization modulators (such as a ferroelectric liquid crystal (FLC)) as both polarization states have to be measured within the timescale that the atmosphere can be considered 'frozen', while dual-beam systems measure both polarization states simultaneously and can therefore handle slow polarization modulators (such as a rotating HWP) as well. When the polarization modulator is downstream of the vAPP, but in front of the polarizer, only dual-beam systems are possible. If the modulator is upstream of the vAPP, both single- and dual-beam systems can be implemented.

The requirements for the components set by [Table 1](#) and [Table 1](#) are sufficient for polarimetric purposes and have been extensively discussed in [section 2](#).

3.1 Implementations for existing instruments

3.1.1 SPHERE-IRDIS

The polarimetric mode of SPHERE-IRDIS³² has been greatly successful in characterizing the scattered NIR light from debris and protoplanetary disks. The polarization modulator of IRDIS is a slowly rotating HWP upstream of the pupil plane where the polarimetric vAPP would be located. The wire grid polarizers are located after the

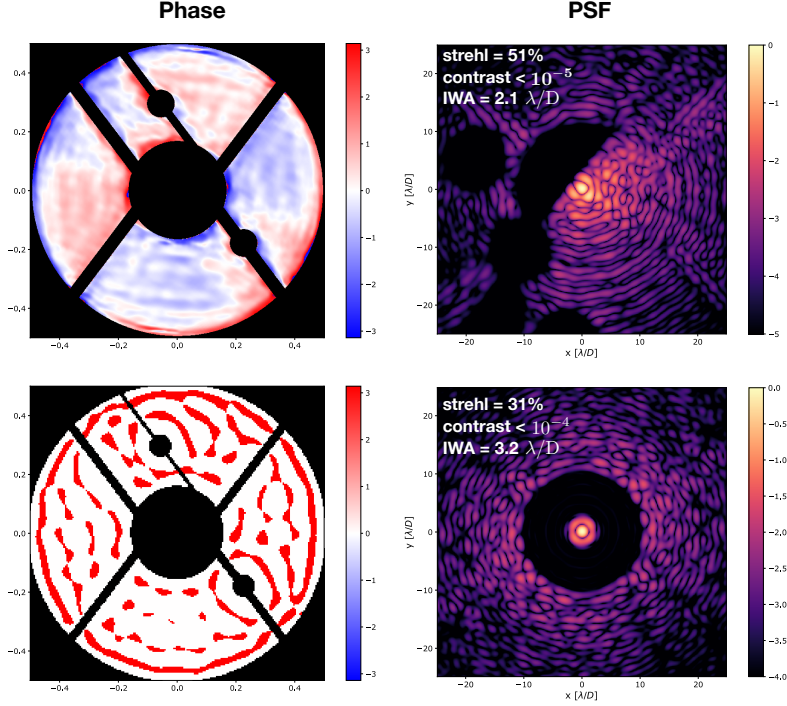


Figure 4. Preliminary 180° ²² (top row) and 360° ¹³ (bottom row) vAPP designs for SCEXAO. Note that the design for the 180° vAPP has been used as well for the SCEXAO gvAPP.²² The SCEXAO vAPP has a more complicated dark hole structure to support phase diversity spots and photometry on the leakage PSF, this might change for the final vAPP design.

beam splitter plate, that ideally would be upgraded to an polarization beam splitting version. The polarimetric vAPP would therefore be a dual-beam 360° vAPP, see Figure 5 A.

3.1.2 SPHERE-ZIMPOL

SPHERE-ZIMPOL,³⁵ operating in visible wavelengths, has a fast polarization modulator (FLC) just before a polarizing beam splitter cube. Unfortunately, there is no pupil plane available between the two components. Therefore, the polarimetric vAPP of choice again is a dual-beam 360° vAPP, see Figure 5 B.

3.1.3 SCEXAO

SCEXAO will be upgraded with an NIR FLC³³ and an Wollaston prism. Down stream of the FLC there would be a pupil plane available where a single-beam 180° vAPP can be installed, as shown in Figure 5 C.

3.1.4 VAMPIRES

VAMPIRES³⁶ is an imaging polarimeter in the visible, that recently got upgraded with an FLC.³³ Between this FLC and the polarizing beam splitter cube is a pupil plane where a single-beam 180° vAPP can be installed, as in Figure 5 C.

3.1.5 SCEXAO gvAPP

SCEXAO already installed a gvAPP in the NIR.²⁹ With the upcoming NIR FLC and Wollaston prism, this can be combined to a narrowband, dual-beam 180° polarimetric vAPP, as shown in Figure 5 D. Note that the other implementations described all are broadband imaging polarimetry implementations.

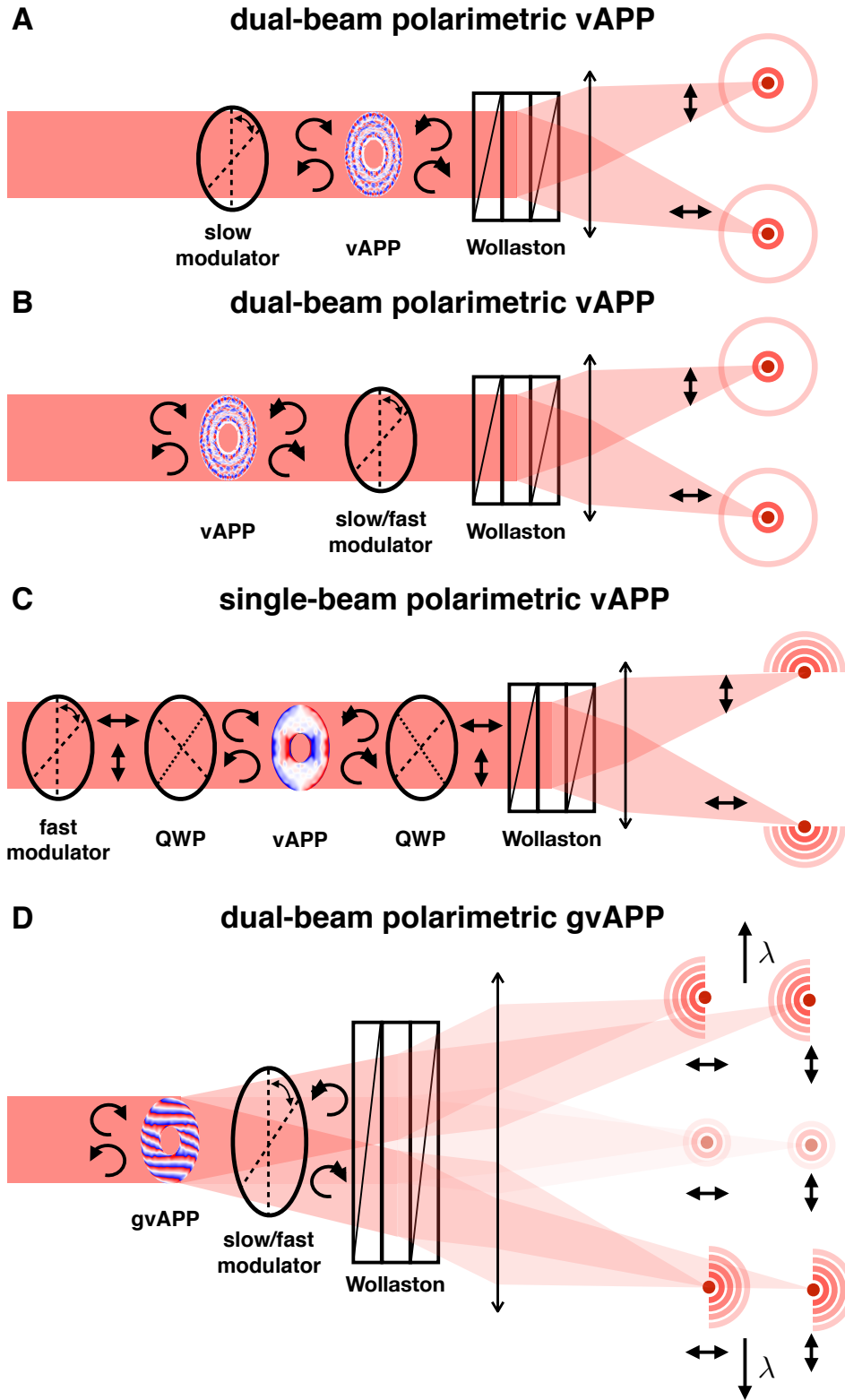


Figure 5. Sketches of several polarimetric vAPP implementations. (A) In case of a slow polarization modulator in front of the coronagraph the solution is an 360° vAPP implementation that enables dual-beam polarimetry. (B) When the polarization modulator (either fast or slow) is located after the coronagraph, again the 360° vAPP is the design of choice. (C) A fast polarization modulator in front of vAPP allows for a single-beam 180° vAPP. (D) A gvAPP followed by a (fast or slow) polarization modulator and a Wollaston prism enables dual-beam narrow band imaging polarimetry with the 180° vAPP.

4. CONCLUSION

We have discussed fully broadband vAPPs that do not suffer from wavelength smearing. We have shown that the symmetry of the coronagraph determines the exact implementation. Symmetric vAPPs can be implemented with the double-grating technique, anti-symmetric vAPPs require an additional QWP and polarizer to split both coronagraphic PSFs. We have set requirements on the components of the vAPP such that the leakage will not limit the raw contrast of 10^{-5} . In the NIR all components are currently available. For the visible and IR wavelengths custom QWPs need to be designed. Further investigation is required to get an overview of all the risks. Furthermore, we have shown that such vAPPs can be installed, with minimal modifications, in the NIR arms of existing high contrast instruments such as SPHERE and SCExAO. Phase designs and the resulting PSFs are presented as well.

Furthermore, we have discussed how polarimetry can be combined with the vAPP. We discussed various implementations, that depend on the symmetry of the coronagraphic PSF, the position and speed of the modulator, and single- or dual-beam polarimetry. We outlined how the polarimetric vAPP could be implemented within SPHERE-IRDIS, SPHERE-ZIMPOL, SCExAO and VAMPIRES.

ACKNOWLEDGMENTS

The research of Steven P. Bos, David S. Doelman, Jos de Boer and Frans Snik leading to these results has received funding from the European Research Council under ERC Starting Grant agreement 678194 (FALCONER). This research used the **hcipy**³⁷ Python package that provides a common framework for performing optical propagation simulations, meant for high contrast imaging.

REFERENCES

- [1] Guyon, O., Martinache, F., Cady, E. J., Belikov, R., Balasubramanian, K., Wilson, D., Clergeon, C. S., and Mateen, M., “How elts will acquire the first spectra of rocky habitable planets,” in [*Adaptive Optics Systems III*], **8447**, 84471X, International Society for Optics and Photonics (2012).
- [2] Marois, C., Lafreniere, D., Doyon, R., Macintosh, B., and Nadeau, D., “Angular differential imaging: a powerful high-contrast imaging technique,” *The Astrophysical Journal* **641**(1), 556 (2006).
- [3] Sparks, W. B. and Ford, H. C., “Imaging spectroscopy for extrasolar planet detection,” *The Astrophysical Journal* **578**(1), 543 (2002).
- [4] Snik, F. and Keller, C. U., “Astronomical polarimetry: polarized views of stars and planets,” in [*Planets, Stars and Stellar Systems*], 175–221, Springer (2013).
- [5] Codona, J. L. and Angel, R., “Imaging extrasolar planets by stellar halo suppression in separately corrected color bands,” *The Astrophysical Journal Letters* **604**(2), L117 (2004).
- [6] Codona, J., Kenworthy, M., Hinz, P., Angel, J., and Woolf, N., “A high-contrast coronagraph for the mmt using phase apodization: design and observations at 5 microns and 2 λ /d radius,” in [*Ground-based and Airborne Instrumentation for Astronomy*], **6269**, 62691N, International Society for Optics and Photonics (2006).
- [7] Kenworthy, M. A., Codona, J. L., Hinz, P. M., Angel, J. R. P., Heinze, A., and Sivanandam, S., “First on-sky high-contrast imaging with an apodizing phase plate,” *The Astrophysical Journal* **660**(1), 762 (2007).
- [8] Guyon, O., Pluzhnik, E., Kuchner, M., Collins, B., and Ridgway, S., “Theoretical limits on extrasolar terrestrial planet detection with coronagraphs,” *The Astrophysical Journal Supplement Series* **167**(1), 81 (2006).
- [9] Snik, F., Otten, G., Kenworthy, M., Miskiewicz, M., Escuti, M., Packham, C., and Codona, J., “The vector-app: a broadband apodizing phase plate that yields complementary psfs,” in [*Modern Technologies in Space-and Ground-based Telescopes and Instrumentation II*], **8450**, 84500M, International Society for Optics and Photonics (2012).
- [10] Pancharatnam, S., “Generalized theory of interference and its applications,” in [*Proceedings of the Indian Academy of Sciences-Section A*], **44**(6), 398–417, Springer (1956).
- [11] Berry, M. V., “The adiabatic phase and pancharatnam’s phase for polarized light,” *Journal of Modern Optics* **34**(11), 1401–1407 (1987).

- [12] Miskiewicz, M. N. and Escuti, M. J., “Direct-writing of complex liquid crystal patterns,” *Optics Express* **22**(10), 12691–12706 (2014).
- [13] Por, E. H., “Optimal design of apodizing phase plate coronagraphs,” in [*Techniques and Instrumentation for Detection of Exoplanets VIII*], **10400**, 104000V, International Society for Optics and Photonics (2017).
- [14] Otten, G. P., Snik, F., Kenworthy, M. A., Miskiewicz, M. N., and Escuti, M. J., “Performance characterization of a broadband vector apodizing phase plate coronagraph,” *Optics Express* **22**(24), 30287–30314 (2014).
- [15] Komanduri, R. K., Kim, J., Lawler, K. F., and Escuti, M. J., “Multi-twist retarders for broadband polarization transformation,” in [*Emerging Liquid Crystal Technologies VII*], **8279**, 82790E, International Society for Optics and Photonics (2012).
- [16] Komanduri, R. K., Lawler, K. F., and Escuti, M. J., “Multi-twist retarders: broadband retardation control using self-aligning reactive liquid crystal layers,” *Optics Express* **21**(1), 404–420 (2013).
- [17] Oh, C. and Escuti, M. J., “Achromatic diffraction from polarization gratings with high efficiency,” *Optics Letters* **33**(20), 2287–2289 (2008).
- [18] Peters-Limbach, M. A., Groff, T. D., Kasdin, N. J., Driscoll, D., Galvin, M., Foster, A., Carr, M. A., LeClerc, D., Fagan, R., McElwain, M. W., et al., “The optical design of charis: an exoplanet ifs for the subaru telescope,” in [*Techniques and Instrumentation for Detection of Exoplanets VI*], **8864**, 88641N, International Society for Optics and Photonics (2013).
- [19] Brandt, T. D., McElwain, M. W., Janson, M., Knapp, G. R., Mede, K., Limbach, M. A., Groff, T., Burrows, A., Gunn, J. E., Guyon, O., et al., “Charis science: performance simulations for the subaru telescope’s third-generation of exoplanet imaging instrumentation,” in [*Adaptive Optics Systems IV*], **9148**, 914849, International Society for Optics and Photonics (2014).
- [20] Claudi, R. U., Turatto, M., Gratton, R. G., Antichi, J., Bonavita, M., Bruno, P., Cascone, E., De Caprio, V., Desidera, S., Giro, E., et al., “Sphere ifs: the spectro differential imager of the vlt for exoplanets search,” in [*Ground-based and Airborne Instrumentation for Astronomy II*], **7014**, 70143E, International Society for Optics and Photonics (2008).
- [21] Mesa, D., Gratton, R., Zurlo, A., Vigan, A., Claudi, R., Alberi, M., Antichi, J., Baruffolo, A., Beuzit, J.-L., Boccaletti, A., et al., “Performance of the vlt planet finder sphere-ii. data analysis and results for ifs in laboratory,” *Astronomy & Astrophysics* **576**, A121 (2015).
- [22] Doelman, D. S., Snik, F., Warriner, N. Z., and Escuti, M. J., “Patterned liquid-crystal optics for broadband coronagraphy and wavefront sensing,” in [*Techniques and Instrumentation for Detection of Exoplanets VIII*], **10400**, 104000U, International Society for Optics and Photonics (2017).
- [23] Otten, G. P., Snik, F., Kenworthy, M. A., Keller, C. U., Males, J. R., Morzinski, K. M., Close, L. M., Codona, J. L., Hinz, P. M., Hornburg, K. J., et al., “On-sky performance analysis of the vector apodizing phase plate coronagraph on magao/clipo2,” *The Astrophysical Journal* **834**(2), 175 (2017).
- [24] Haffert, S. Y., Wilby, M. J., Keller, C. U., Snellen, I. A. G., Doelman, D. S., Por, E. H., Wardenier, J., and Fagginger Auer, F., “On-sky results of high-dispersion integral-field spectroscopy and high-contrast imaging with the leiden exoplanet instrument(lexi),” in [*Adaptive Optics Systems VI*], **10703**, International Society for Optics and Photonics (2018).
- [25] Snellen, I., de Kok, R., Birkby, J., Brandl, B., Brogi, M., Keller, C., Kenworthy, M., Schwarz, H., and Stuik, R., “Combining high-dispersion spectroscopy with high contrast imaging: Probing rocky planets around our nearest neighbors,” *Astronomy & Astrophysics* **576**, A59 (2015).
- [26] Beuzit, J.-L., Feldt, M., Dohlen, K., Mouillet, D., Puget, P., Wildi, F., Abe, L., Antichi, J., Baruffolo, A., Baudoz, P., et al., “Sphere: a planet finder instrument for the vlt,” in [*Ground-based and airborne instrumentation for astronomy II*], **7014**, 701418, International Society for Optics and Photonics (2008).
- [27] Jovanovic, N., Martinache, F., Guyon, O., Clergeon, C., Singh, G., Kudo, T., Garrel, V., Newman, K., Doughty, D., Lozi, J., et al., “The subaru coronagraphic extreme adaptive optics system: enabling high-contrast imaging on solar-system scales,” *Publications of the Astronomical Society of the Pacific* **127**(955), 890 (2015).

- [28] Skrutskie, M., Jones, T., Hinz, P., Garnavich, P., Wilson, J., Nelson, M., Solheid, E., Durney, O., Hoffmann, W., Vaitheeswaran, V., et al., “The large binocular telescope mid-infrared camera (Imircam): final design and status,” in [*Ground-based and Airborne Instrumentation for Astronomy III*], **7735**, 77353H, International Society for Optics and Photonics (2010).
- [29] Doelman, D. S., Por, E. H., Bos, S. P., Lozi, J., Guyon, O., Jovanovic, N., Groff, T. D., Warriner, N. Z., Escuti, M. J., and Snik, F., “First light for the vapp on scexao/charis,” in [*Adaptive Optics Systems VI*], **10703**, International Society for Optics and Photonics (2018).
- [30] Fusco, T., Rousset, G., Sauvage, J.-F., Petit, C., Beuzit, J.-L., Dohlen, K., Mouillet, D., Charton, J., Nicolle, M., Kasper, M., et al., “High-order adaptive optics requirements for direct detection of extrasolar planets: Application to the sphere instrument,” *Optics Express* **14**(17), 7515–7534 (2006).
- [31] Dohlen, K., Langlois, M., Saisse, M., Hill, L., Origine, A., Jacquet, M., Fabron, C., Blanc, J.-C., Llored, M., Carle, M., et al., “The infra-red dual imaging and spectrograph for sphere: design and performance,” in [*Ground-based and Airborne Instrumentation for Astronomy II*], **7014**, 70143L, International Society for Optics and Photonics (2008).
- [32] Langlois, M., Dohlen, K., Vigan, A., Zurlo, A., Moutou, C., Schmid, H., Mili, J., Beuzit, J.-L., Boccaletti, A., Carle, M., et al., “High contrast polarimetry in the infrared with sphere on the vlt,” in [*Ground-based and Airborne Instrumentation for Astronomy V*], **9147**, 91471R, International Society for Optics and Photonics (2014).
- [33] Lozi, J., Guyon, O., and et al., “Scexao, an instrument with a dual purpose: perform cutting-edge science and develop new technologies,” in [*Adaptive Optics Systems VI*], **10703**, International Society for Optics and Photonics (2018).
- [34] Snik, F., Otten, G., Kenworthy, M., Mawet, D., and Escuti, M., “Combining vector-phase coronagraphy with dual-beam polarimetry,” in [*Ground-based and Airborne Instrumentation for Astronomy V*], **9147**, 91477U, International Society for Optics and Photonics (2014).
- [35] Thalmann, C., Schmid, H. M., Boccaletti, A., Mouillet, D., Dohlen, K., Roelfsema, R., Carbillet, M., Gisler, D., Beuzit, J.-L., Feldt, M., et al., “Sphere zimpol: overview and performance simulation,” in [*Ground-based and Airborne Instrumentation for Astronomy II*], **7014**, 70143F, International Society for Optics and Photonics (2008).
- [36] Norris, B., Schworer, G., Tuthill, P., Jovanovic, N., Guyon, O., Stewart, P., and Martinache, F., “The vampires instrument: imaging the innermost regions of protoplanetary discs with polarimetric interferometry,” *Monthly Notices of the Royal Astronomical Society* **447**(3), 2894–2906 (2015).
- [37] Por, E. H., Haffert, S. Y., Radhakrishnan, V. M., Doelman, D. S., Van Kooten, M., and Bos, S. P., “High contrast imaging for python (hcpy): an open-source adaptive optics and coronagraph simulator,” in [*Adaptive Optics Systems VI*], **10703**, International Society for Optics and Photonics (2018).